Molecular Biology of the Cell
Vol. 18, 4780–4793, December 2007

Interaction of Ezrin with the Novel Guanine Nucleotide Exchange Factor PLEKHG6 Promotes RhoG-dependent Apical Cytoskeleton Rearrangements in Epithelial Cells

Romina D'Angelo,*† Sandra Aresta,‡ Anne Blangy,§ Laurence Del Maestro,*† Daniel Louvard,*† and Monique Arpin*†

*Centre National de la Recherche Scientifique, Unité Mixte de Recherche 144, Paris 75248, France; †Institut Curie, Centre de Recherche, Paris 75248, France; ‡Hybrigenics, 75014 Paris, France; and §Centre National de la Recherche Scientifique, Centre de Recherche de Biochimie Macromoléculaire, 34293 Montpellier Cedex 5, France

Submitted December 22, 2006; Revised July 18, 2007; Accepted September 11, 2007
Monitoring Editor: Martin A. Schwartz

The mechanisms underlying functional interactions between ERM (ezrin, radixin, moesin) proteins and Rho GTPases are not well understood. Here we characterized the interaction between ezrin and a novel Rho guanine nucleotide exchange factor, PLEKHG6. We show that ezrin recruits PLEKHG6 to the apical pole of epithelial cells where PLEKHG6 induces the formation of microvilli and membrane ruffles. These morphological changes are inhibited by dominant negative forms of RhoG. Indeed, we found that PLEKHG6 activates RhoG and to a much lesser extent Rac1. In addition we show that ezrin forms a complex with PLEKHG6 and RhoG. Furthermore, we detected a ternary complex between ezrin, PLEKHG6, and the RhoG effector ELMO. We demonstrate that PLEKHG6 and ezrin are both required in macropinocytosis. After down-regulation of either PLEKHG6 or ezrin expression, we observed an inhibition of dextran uptake in EGF-stimulated A431 cells. Altogether, our data indicate that ezrin allows the local activation of RhoG at the apical pole of epithelial cells by recruiting upstream and downstream regulators of RhoG and that both PLEKHG6 and ezrin are required for efficient macropinocytosis.

INTRODUCTION

The membrane-cytoskeleton linker ezrin is mainly expressed in epithelial cells where it associates to the apical actin-rich structures such as microvilli (Berryman *et al.*, 1993, 1995). Recent genetic analyses revealed that ezrin is essential for the morphogenesis of epithelial cells (Fiévet *et al.*, 2007). In ezrin$^{-/-}$ mice, morphological defects in the apical domain of intestinal and retinal pigment epithelial cells have been observed (Saotome *et al.*, 2004; Bonilha *et al.*, 2006). In parietal cells, ezrin knockdown impairs the formation of canalicular apical membrane, resulting in severe achlorhydria (Tamura *et al.*, 2005).

How ezrin participates in the assembly of the apical actin-rich structures such as microvilli is still poorly understood. The association of ezrin and the highly related proteins radixin and moesin with the cortical actin cytoskeleton is strictly regulated. ERM (ezrin, radixin, moesin) proteins contain a conserved globular N-terminal domain, called the FERM domain (Four point one ezrin, radixin, moesin), involved in the binding to both phosphatidylinositol 4,5 bisphosphate (PIP_2; Barret *et al.*, 2000) and plasma membrane proteins and a C-terminal F-actin–binding domain that resides in the last 34 amino acids (Turunen *et al.*, 1994; Bretscher *et al.*, 2002). In the cytoplasm, ERM proteins exist in a closed conformation because of an intramolecular interaction between the N-terminal domain and the last 100 amino acids called N- and C-ERMAD (ERM association domain), respectively (Gary and Bretscher, 1995). This intramolecular association masks the binding sites for plasma membrane proteins and F-actin. An activation step is required to disrupt this association that occurs through conformational changes induced by sequential binding to PIP_2 and phosphorylation of a conserved C-terminal threonine residue (T567 in ezrin; Matsui *et al.*, 1998; Fiévet *et al.*, 2004).

A link between the signaling pathways triggered by the small GTPases of the Rho family and activation of ERM proteins has been suggested. The ability of ERM proteins to bind the cytoplasmic domain of CD44 is increased by activation of Rho (Hirao *et al.*, 1996). In permeabilized fibroblasts, ERM proteins are required for the formation of focal adhesions and actin stress fibers in response to active RhoA and Rac (Mackay *et al.*, 1997). A RhoA-dependent activation mechanism for ERM proteins has been proposed on the basis that overexpression of either RhoA or its direct effector, the phosphatidylinositol 4-phosphate 5-kinase, results in the elevation of PIP_2 and induction of microvilli with a concomitant recruitment of activated ERM proteins (Hirao *et al.*, 1996; Matsui *et al.*, 1999; Yonemura *et al.*, 2002). However,

This article was published online ahead of print in *MBC in Press* (http://www.molbiolcell.org/cgi/doi/10.1091/mbc.E06–12–1144) on September 19, 2007.

Address correspondence to: Monique Arpin (marpin@curie.fr).

Abbreviations used: DH, Dbl-homology; EGF, epidermal growth factor; ERM, ezrin, radixin, moesin; GDI, guanine dissociation inhibitor; GEF, guanine nucleotide exchange factor; GFP, green fluorescent protein; GST, glutathione *S*-transferase; PH, pleckstrin homology; PLEKHG6, pleckstrin homology domain containing, family G (with RhoGef domain) member 6; TRITC-dextran, tetramethylrhodamine isothiocyanate-dextran.

Rac1 activation in T-lymphocytes by chemokine or after TCR engagement leads to ERM protein inactivation with a concomitant microvillus breakdown (Faure *et al.*, 2004; Nijhara *et al.*, 2004). These observations suggest that Rho GTPases can function as upstream regulators of ERM proteins.

However, in vitro and in vivo studies have indicated that ERM proteins can act as upstream regulators of Rho GTPases by binding to the Rho GDP dissociation inhibitor (RhoGDI). This association is thought to displace RhoGDI from Rho GTPases, allowing them to be activated by their specific guanine nucleotide exchange factors (GEFs; Takahashi *et al.*, 1997). An association of ERM proteins with the exchange factor Dbl in vitro as well as in vivo has been reported (Takahashi *et al.*, 1998; Lee *et al.*, 2004; Vanni *et al.*, 2004). In epithelial cells, an active form of ezrin has been shown to activate the small GTPase Rac1 with a concomitant disassembly of adherens junctions (Pujuguet *et al.*, 2003). A genetic analysis in *Drosophila*, however, has suggested that *Drosophila* moesin negatively regulates the *Rho1* pathway (Speck *et al.*, 2003). Therefore, these data reveal a complex relationship between ERM proteins and the small GTPases, supporting the idea that ERM proteins function both upstream and downstream of Rho GTPases.

Using a yeast two-hybrid screen we identified a novel GEF that interacts with ezrin and that activates the small GTPase RhoG. RhoG shares significant homology with Rac1 (72% identity) and is believed to function upstream of Rac1 and Cdc42 (Gauthier-Rouviere *et al.*, 1998; Katoh *et al.*, 2000, 2006). However, other studies suggest that RhoG signals in parallel of Rac1 and Cdc42 rather than upstream (Wennerberg *et al.*, 2002; Prieto-Sanchez and Bustelo, 2003). Although several regulators of the RhoA, Rac1 and Cdc42 GTPases have been characterized few regulators of RhoG have been identified. As a consequence the processes controlled by activated RhoG are poorly understood. Trio, through its N-terminal DH/PH tandem, functions as a RhoG exchange factor and activation of RhoG by TrioGEF1 regulates neurite outgrowth (Blangy *et al.*, 2000; Katoh *et al.*, 2000; Estrach *et al.*, 2002). SGEF, another exchange factor for RhoG, stimulates macropinocytosis in fibroblasts (Ellerbroek *et al.*, 2004). Recent studies have identified ELMO as a specific effector of RhoG (Katoh and Negishi, 2003). ELMO has been implicated in cell migration, in phagocytosis of apoptotic cells, and in RhoG-mediated neurite outgrowth (Gumienny *et al.*, 2001; Wu *et al.*, 2001; Katoh and Negishi, 2003; deBakker *et al.*, 2004; Grimsley *et al.*, 2004). In these processes, ELMO cooperates with Dock180 to promote downstream Rac activation. Furthermore, an interaction between ERM proteins and ELMO has recently been reported (Grimsley *et al.*, 2006).

Here we characterize the interaction between ezrin and a novel GEF, PLEKHG6 (pleckstrin homology domain containing family G with RhoGef domain member 6). PLEKHG6 displays an exchange activity toward RhoG and to a much lesser extent toward Rac1. We show that ezrin recruits PLEKHG6 to the apical surface of epithelial cells where it promotes the activation of RhoG. In addition to its interaction with PLEKHG6 and RhoG, ezrin also forms a ternary complex with PLEKHG6 and the RhoG effector ELMO, indicating that ezrin interacts with upstream and downstream regulators of RhoG. We demonstrate that the interaction of ezrin with PLEKHG6 is critical for PLEKHG6-induced morphological changes at the apical surface of epithelial cells but is not necessary for its catalytic activity. Moreover, we show that both ezrin and PLEKHG6 are required for macropinocytosis in epidermal growth factor (EGF)-stimulated A431 cells.

MATERIALS AND METHODS

Antibodies and Reagents

A rabbit polyclonal antibody anti-PLEKHG6 was generated against the peptide AGESPWESSGEEEE (aa 704-717) coupled to a carboxyl cysteine residue and affinity-purified against the same peptide. The following antibodies were used: affinity-purified rabbit polyclonal anti-vesicular stomatitis virus glycoprotein epitope (VSVG) and anti-ezrin antibodies (Gautreau *et al.*, 2000); monoclonal anti-VSVG antibody (clone P5D4; Kreis, 1986); mouse monoclonal anti-Myc (clone 9E10); and affinity-purified rabbit polyclonal anti-green fluorescent protein (GFP) antibodies were raised in the laboratory; rat monoclonal anti-HA (clone 3F10) and mouse monoclonal anti-GFP were from Roche (Meylan, France); mouse monoclonal anti-Rac1, Upstate Biotechnology (Lake Placid, NY); mouse monoclonal anti-α tubulin, Sigma-Aldrich (L'Isle D'Abeau Chesnes, France); rabbit polyclonal anti-Cdc42, Santa Cruz Biotechnology (Santa Cruz, CA). Horseradish peroxidase–conjugated goat anti-rabbit, anti-mouse and anti-rat secondary antibodies were from Jackson ImmunoResearch Laboratories (Soham, United Kingdom). Cy3- and Alexa 488–conjugated goat anti-rabbit and anti-mouse antibodies were from Jackson ImmunoResearch Laboratories. Rhodamine-phalloidin and Alexa Fluor 350 phalloidin were from Molecular Probes (Invitrogen, Carlsbad, CA). Glutathione-Sepharose 4B beads and protein A-Sepharose fast-flow beads were purchased from Amersham Pharmacia Biotech (Uppsala, Sweden). Tetramethylrhodamine isothiocyanate-dextran (TRITC-Dextran; 155,000 average mol wt) was purchased from Sigma-Aldrich. EGF was from BD Biosciences (Bedford, MA).

Plasmids

A cDNA for human PLEKHG6 (FLJ10665, Accession number NP_060643) was obtained from the National Institute of Technology and Evaluation (Japan). For expression in mammalian cells, cDNAs encoding the different Myc-tagged PLEKHG6 were inserted into the pcDNA3.1 vector (Invitrogen). Point mutations were generated by site-directed mutagenesis (QuickChange; Stratagene, La Jolla, CA). Ezrin plasmids for eukaryotic expression and GST-tagged ezrin plasmids were previously described (Gautreau *et al.*, 2000; Srivastava *et al.*, 2005). Hemagglutinin (HA)-tagged RhoG (wt and Q61L), GFP-tagged RhoG (T17N and F37A), and GFP-tagged Rac1(T17N) were a gift from Dr. P. Fort (Centre de Recherche de Biochimie Macromoléculaire, Montpellier, France). Myc-tagged Rac1(Q61L) and Cdc42(Q61L) were from Dr. A. Hall (Memorial Sloan-Kettering Cancer Center). The Pak CRIB-encompassing domain (amino acids 70–118) fused to glutathione *S*-transferase (GST) was from Dr. Lowe (GlaxoSmithKline, United Kingdom) (Thompson *et al.*, 1998). GFP-tagged and GST-tagged ELMO plasmids were provided by Dr. K. Ravichandran (University of Virginia, Charlottesville, VA).

Yeast Two-Hybrid Screen

Yeast two-hybrid screens were performed with ezrin fragments as baits to screen a random-primed cDNA library from human placenta using a previously described mating protocol (Formstecher *et al.*, 2005).

Cell Culture and Transfection

LLC-PK1 (CCL 101; American Type Culture Collection, Manassas, VA), JEG-3 (ACC463; DSMZ, Braunschweig, Germany), and the human epidermoid carcinoma A431 cells were maintained in DMEM containing 10% fetal bovine serum (FBS) under 10% CO_2 at 37°C. LLC-PK1 cells stably transfected with the vector alone (pcB6), with cDNA coding for VSVG-tagged wt ezrin (clone E17) or VSVG-tagged ezrin T567D (clone D2) have previously been described (Gautreau *et al.*, 2000). LLC-PK1 and NIH3T3 cells were transfected by electroporation as described previously (Gautreau *et al.*, 2000). Transiently transfected cells were analyzed after 20 h of cDNA expression. 293T cells (2×10^6) were transiently transfected by the calcium phosphate method (Wigler *et al.*, 1977) and analyzed 24 or 48 h after transfection.

Northern Blot

A premade Northern blot containing poly A^+ RNA from different human tissues (Human 12-lane MTN Blot; Clontech-BD Biosciences; Palo Alto, CA) was hybridized with a PCR-amplified fragment of PLEKHG6 cDNA corresponding to nucleotides 1885–2518 and labeled with [α-^{32}P]CTP using the Megaprime DNA Labeling System (Amersham Pharmacia Biotech).

In Vitro Transcription/Translation Assay

Transcription and translation reactions were performed using the TNT Coupled Reticulocyte Lysate System according to the manufacturer's instructions (Promega, Madison, WI). Briefly, transcription of PLEKHG6-CT fragment (aa 579-790) was obtained using a PCR fragment as template amplified from PLEKHG6 cDNA carrying the 3′ UTR (untranslated region). Primers used are the following: 5′CTTAATACGACTCACTATAGGGAAACAGACACCATGCTTGTGCCAGATGATACCTCAGAC-3′carrying the T7 promoter sequence followed by the Kozak sequence, and 5′-CGACCTGCAGCTCGAGCACA-3′ was designed to include the 3′UTR. Translation was performed in the presence of [^{35}S]methionine (Amersham Pharmacia Biotech).

The GST-pulldown assays were performed by incubating equal amounts of GST or GST fusion proteins immobilized to glutathione-Sepharose beads (Amersham Pharmacia Biotech) with 5 μl of ^{35}S-labeled protein mixture in a final volume of 100 μl of binding buffer (20 mM sodium phosphate, pH 6, 150 mM NaCl, 10% glycerol, 1 mM phenylmethylsulfonyl fluoride (PMSF), 1 mM dithiothreitol, 0.02% (vol/vol) Nonidet P-40) for 3 h at room temperature. Beads were washed three times with binding buffer, and bound proteins were eluted in Laemmli sample buffer, run on SDS-PAGE (15%), and visualized by autoradiography.

Pulldowns

293T cells transfected with the indicated plasmids were lysed with RIPA buffer (50 mM HEPES, pH 7.2, 10 mM EDTA, 150 mM NaCl, 1% (vol/vol) Nonidet P-40, 0.5% Na sodium deoxycholate (DOC), 0.1% SDS, 10 μg/ml pepstatin, 10 μg/ml aprotinin, 10 μg/ml leupeptin, and 1 mM PMSF). Clarified lysates were incubated with GST fusion proteins (20–30 μg) bound to glutathione-Sepharose beads for 3 h at 4°C. Beads were washed three times with lysis buffer, and bound proteins were eluted in Laemmli sample buffer and separated by SDS-PAGE. For the competition assay-purified ezrin-CT was added to the lysates and incubated for 3 h at 4°C with GST-ezrin-NT immobilized on glutathione-Sepharose beads. The amount of purified GST-ezrin-CT used was four times the amount of GST-ezrin-NT.

Immunoprecipitation and Immunoblotting

293T cells transfected with the indicated plasmids were lysed with RIPA buffer for 10 min. Clarified lysates from 293T cells were incubated with 2 μg of rabbit polyclonal antibodies (anti-VSVG or anti-GFP), together with protein A-Sepharose for 3 h at 4°C. Beads were processed as described above. All blots were performed on nitrocellulose membranes (Protran Hybond; Whatman, Dassel, Germany) and developed using horseradish peroxidase-conjugated secondary antibodies and an ECL detection kit (Amersham Pharmacia Biotech).

GTPase Activity Assays

LLC-PK1 cells transfected with the indicated plasmids were lysed with ice-cold lysis buffer (50 mM Tris pH 7.2, 1% Triton X-100, 0.5% Na DOC, 0.1% SDS, 500 mM NaCl, 10 mM $MgCl_2$, 10 μg/ml pepstatin, 10 μg/ml aprotinin, 10 μg/ml leupeptin, and 1 mM PMSF). Bacterially produced GST-ELMO (100 μg) and GST-CRIB (20 μg) proteins bound to glutathione-Sepharose beads were incubated with lysates from LLC-PK1 cells for 1 h at 4°C. The beads were washed four times with washing buffer (50 mM Tris pH 7.2, 1% Triton X-100, 150 mM NaCl, 10 mM $MgCl_2$, 10 μg/ml pepstatin, 10 μg/ml aprotinin, 10 μg/ml leupeptin, and 1 mM PMSF). The bound proteins were eluted in Laemmli sample buffer and separated by SDS- PAGE (15%). Densitometric analyses were performed with Scion Image (Frederick, MD).

Yeast Exchange Activity

The LexA, GAL4, TRIO-GEFD1, and βPIX constructs have been reported earlier (De Toledo *et al.*, 2000). Complementary DNAs coding for PLEKHG6 domains fused to the Myc tag were inserted into the yeast expression vector pRs426Met (Tirode *et al.*, 1997). Interactions were assayed in yeast strain TAT7 [Mata, trp1, his3, leu2, ura3, ade2, and LYS:(LexAop)8-lacZ] provided by Jacques Camonis, Institut Curie, Paris, France). Filter assays for β-galactosidase activity were performed as described (De Toledo *et al.*, 2000).

Down-Regulation of Ezrin and PLEKHG6 by shRNA

For ezrin and PLEKHG6 silencing, A431 cells were transfected with the psiRNA-h7SK-GFPzeo vector to generate short hairpin RNA (shRNA) and the reporter GFP (Invivogen). The following oligonucleotides were used to target ezrin human sequence: Ez1 (coding sequence nucleotides 711-731) 5′ ACCTCGATTGGCTTTCCTTGGAGTGATCAAGAGTCACTCCAAGGAA-AGCCAATCTT3′ and Ez2 (coding sequence nucleotides 326-346) 5′AC-CTCGAATCCTTAGCGATGAGATCTTCAAGAGAGATCTCATCGCT-AAGGATTCTT3′. The following oligonucleotides were used to target PLEKHG6 human sequence: Sequence 1 (nucleotides 1178-1198) 5′ACCTCGGAGT-CATTCCTGCGACATATTCAAGAGATATGTCGCAGGAATGACTCCTT and Sequence 2 (nucleotides 1691-1711) 5′ACCTCGAAGGCAGAGGAG-TATGTTCATCAAGAGTGAACATACTCCTCTGCCTTCTT3′. The sequence of scramble nucleotides (Scr) used was as follows: 5′ACCTCGATATGTGCGTAC-CTAGCATTCAAGAGATGCTAGGTACGCACATATTT3′. A431 cells were transfected with plasmid small interfering RNA (psiRNA) plasmids using Lipofectamine 2000 according to the manufacturer's instructions (Invitrogen).

RT-PCR

Total RNA, 2 μg, extracted from A431 cells transfected with scramble or PLEKHG6 psiRNA were used for the first-stand cDNA synthesis with the SuperScript reverse transcriptase according to the manufacturer's instructions (Invitrogen). Semiquantitative PCR was performed using, in the same reaction, the following oligos: PLEKHG6f: 5′CCACCCTGGACCTGACGTCC. PLEKHG6r: 5′TCAGTGGCCAGCTTTCAGGAACAGAG. GADPHf: 5′CCT-CAACTACAGGTCTACA3′. GADPHr: 5′TTCTCGTGGTTCACACCCAT3′.

Macropinocytosis Assay

After transfection with psiRNAs, A431 cells were cultured for 3 d on glass coverslips. Before the macropinocytosis assay, cells were incubated for 3 h in serum-free DMEM medium plus 1 mM HEPES and 0.15% BSA. Cells were then incubated at 37°C for 5 min in the same medium containing 1 mg/ml TRITC-dextran and 100 ng/ml EGF. The cells were then quickly rinsed with ice-cold PBS, fixed with 4% paraformaldehyde, and processed for fluorescence.

Immunofluorescence

After fixation with 4% paraformaldehyde, cells were permeabilized with 0.5% Triton X-100 for 5 min and incubated with primary and secondary antibodies. Cells were examined using an epifluorescence microscope (DM 6000B Leica, Deerfield, IL) coupled to a CCD camera (Cool Snap, Roper Scientific, Tucson, AZ). Images were analyzed using Metaview Software (Universal Imaging, West Chester, PA).

RESULTS

Identification of PLEKHG6, a Novel GEF That Interacts with Ezrin

In yeast two-hybrid screens performed with ezrin constructs as baits, we identified an uncharacterized protein corresponding to a putative GEF. Seven independent clones were isolated that cover a region corresponding to the carboxy-terminal part (aa 579-790) of the hypothetical protein FLJ10665 (UniGene: PLEKHG6; Figure 1A). These clones were found in two independent screens performed with either the amino-terminal domain of ezrin (aa 1-310) or ezrin truncated of the last 52 amino acids as baits but not with full-length ezrin.

The open reading frame of this gene predicts a protein of 790 amino acids. A search for conserved domains in the protein identified a Dbl homology domain (DH) followed by a pleckstrin homology domain (PH; Figure 1A). No other known functional domains or motifs have been identified in either the N- or the C-terminal regions. Accordingly to the Unigene nomenclature we will refer to this novel RhoGEF as PLEKHG6. Alignment of the PLEKHG6 DH domain sequence with that of known GEFs showed significant homology with the DH domain of human GEF720 (48% identity, 64% similarity), an uncharacterized Dbl-related protein from *Drosophila melanogaster* (CG7323; 36% identity, 55% similarity) and *Caenorhabditis elegans* (T08H4.1; 31% identity, 55% similarity; Figure 1B). Phylogenetic trees based on the sequence of DH domains from human Dbl family members indicate that GEF720 and PLEKHG6 belong to the same subgroup (tree branch; Schmidt and Hall, 2002; Rossman *et al.*, 2005). The PH domain of PLEKHG6 shows also significant homology with the PH domain of GEF720 (53% identity, 75% similarity), with the putative PH domains of CG7323 (36% identity, 54% similarity) and T08H4.1 (34% identity, 60% similarity; Figure 1B).

Northern blot analysis of PLEKHG6 mRNA expression revealed that the highest expression level was in human placenta (Figure 1C). A low mRNA level was also observed in small intestine, lung, liver, kidney, thymus, and heart. In agreement with the predicted molecular weight, a protein with a relative molecular mass of 89 kDa was immunoprecipitated from lysates of human choriocarcinoma JEG-3, porcine kidney LLC-PK1, and human epidermoïd A431 cells using an antibody raised against a peptide located in the carboxy-terminal region of PLEKHG6 (Figure 1D). However, only the overexpressed PLEKHG6 but not the endogenous protein was detected by Western blot with this antibody in the total cellular lysate (Figure 1D). These results indicate that PLEKHG6 is expressed in very low amounts both at the mRNA and protein levels.

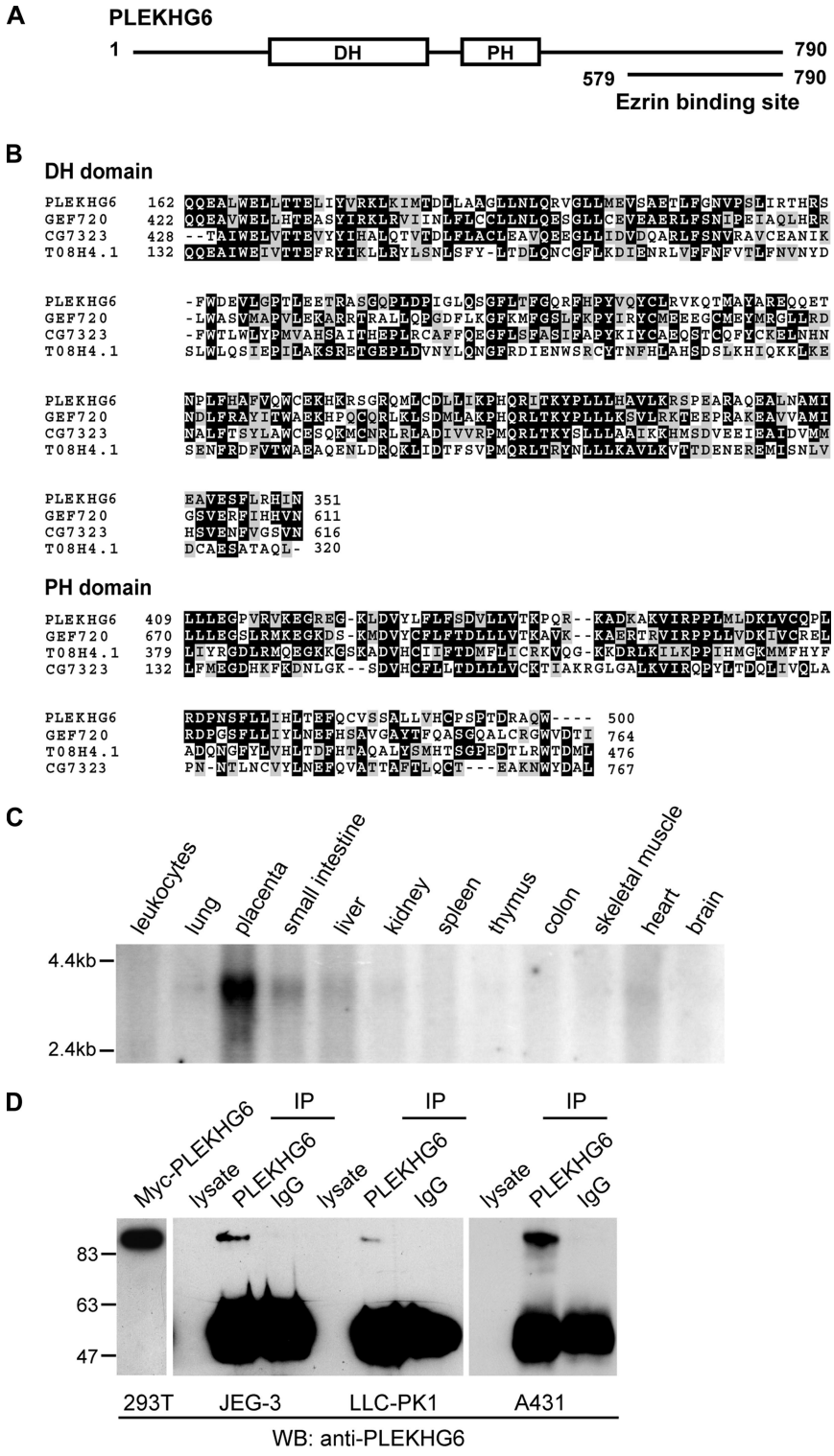

Figure 1. Structural organization and expression pattern of human PLEKHG6. (A) PLEKHG6 contains a Dbl homology domain (DH) followed by a plekstrin homology (PH) domain. The bar represents the longest cDNA isolated in the yeast two-hybrid screen that encodes the ezrin binding site (aa 579-790). (B) Sequence comparison of DH and PH domains from PLEKHG6, human GEF720 (Acc. no BAA34440), *D. melanogaster* CG7323 (Acc. no NP_649182), and *C. elegans* T08H4.1 (Acc. no NP_494723). Black and gray letters indicate identical and conserved amino acids, respectively. (C) Northern blot analysis of PLEKHG6 mRNA expression in human tissues. A single band at ~3 kb was detected. (D) PLEKHG6 is expressed in JEG-3, LLC-PK1, and A431 cells. Cells lysates from JEG-3, LLC-PK1, and A431 cells were immunoprecipitated with an anti-PLEKHG6 antibody and immunoblotting on total cell lysates, and immunoprecipitates was performed with the same antibody. Lane 1, lysate from 293T cells transfected with Myc-PLEKHG6 used as control.

The C-terminal Region of PLEKHG6 Interacts with the N-terminal Domain of Ezrin

The interaction between PLEKHG6 and ezrin found in the yeast two-hybrid screen was confirmed using different approaches. First, the C-terminal region of PLEKHG6 (aa 579-790) was synthesized in vitro and incubated with various forms of bacterially purified GST-ezrin (Figure 2A). As shown in Figure 2B the C-terminal fragment of PLEKHG6 interacts with the N-terminal domain of ezrin as well as with ezrin deleted of the last 52 amino-acids (ezrin-Δ52) but not with the C-terminal domain of ezrin. To further analyze the interacting domains between ezrin and PLEKHG6, we performed pull-downs with various forms of GST-ezrin and lysates of 293T cells expressing different Myc-tagged forms of PLEKHG6 (Figure 2, A and C). We found that GST-ezrin-NT pulled down efficiently PLEKHG6-wt and PLEKHG6-ΔNT but not

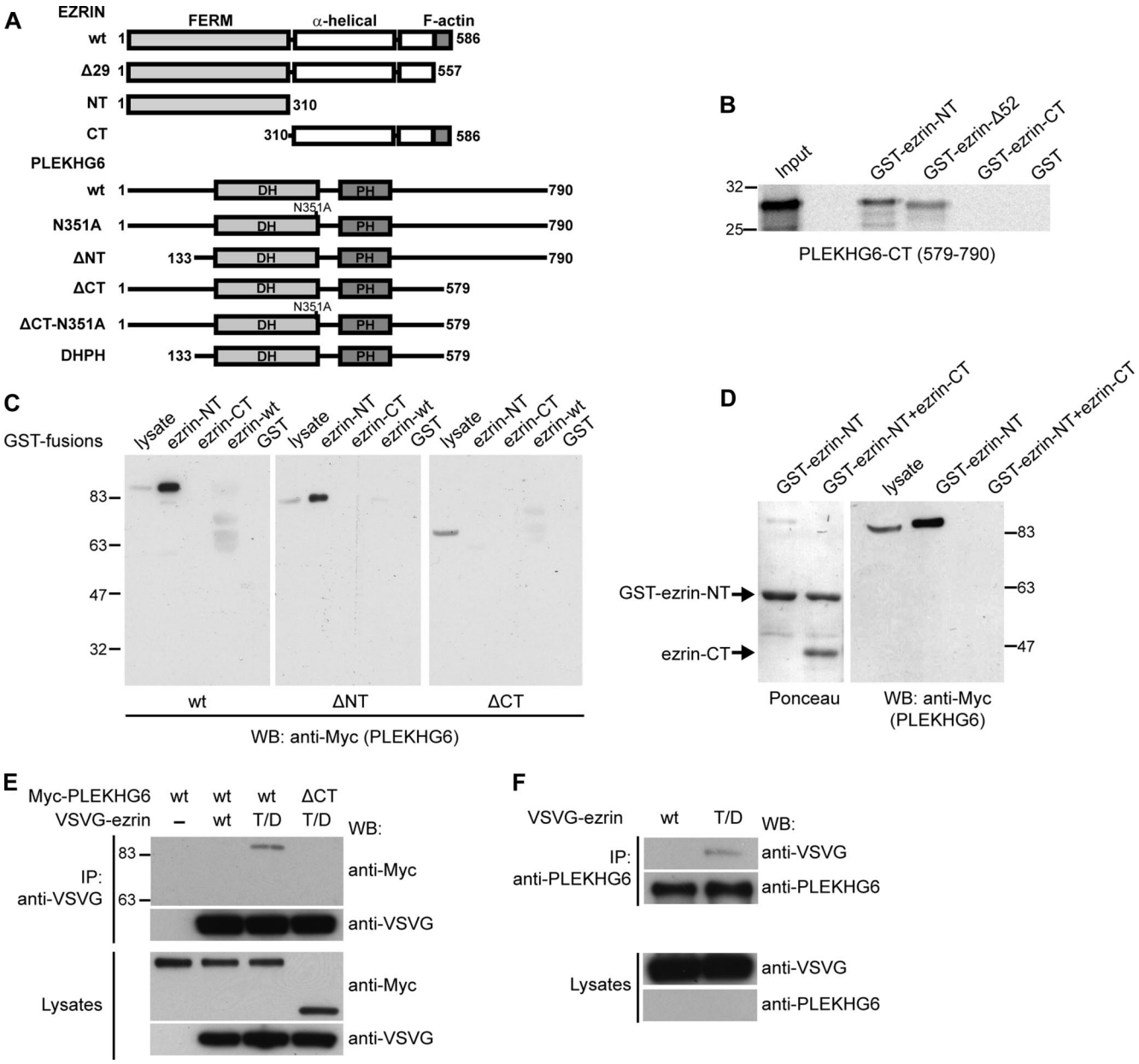

Figure 2. The C-terminal region of PLEKHG6 interacts with the N-terminal domain of ezrin. (A) Schematic representation of the domain structures of ezrin and PLEKHG6 and of the different forms used in the experiments. Ezrin contains a globular amino-terminal domain (FERM domain) followed by an α-helical region and a F-actin–binding site. (B) ^{S35}Met-labeled PLEKHG6-CT produced by in vitro transcription/translation was incubated with either GST or GST-fused ezrin constructs. The translation product corresponding to PLEKHG6-CT used in each reaction (input) or bound to GST-ezrin constructs was visualized by autoradiography. (C) PLEKHG6-wt and -ΔNT interact only with ezrin-NT. GST or GST-fused ezrin constructs immobilized on glutathione beads were incubated with lysates from 293T cells expressing Myc-tagged PLEKHG6-wt, -ΔNT, and -ΔCT. Bound PLEKHG6 proteins were detected by Western blot with an anti-Myc antibody. (D) PLEKHG6 binding site on ezrin is cryptic. 293T cell lysates expressing Myc-tagged PLEKHG6 were incubated with GST-ezrin-NT in the presence or not of ezrin-CT. Left panel, ponceau staining of GST-ezrin-NT and ezrin-CT. Right panel, Western blot with anti-Myc antibody. Addition of the purified ezrin-CT in the pulldown assay prevents the association of PLEKHG6 with GST-ezrin-NT. (E) PLEKHG6 coimmunoprecipitates with ezrin T567D. LLC-PK1 cells stably transfected with the vector (−), the cDNAs coding for wild-type ezrin (wt) or for ezrin T567D (T/D) were transiently transfected with the plasmids encoding either Myc-tagged PLEKHG6-wt or -ΔCT. Immunoprecipitation was performed with an anti-VSVG antibody (top panel). Western blot was performed with anti-Myc or anti-VSVG antibodies on immunoprecipitated proteins (top panel) and on cell lysates (bottom panels). (F) Endogenous PLEKHG6 immunoprecipitates ezrin T567D. Immunoprecipitation with an anti-PLEKHG6 antibody was performed in LLC-PK1 cells stably expressing VSVG-tagged ezrin wt or T567D. Western blot was performed with anti-VSVG and anti-PLEKHG6 on immunoprecipitated proteins (top panel) and cell lysates (bottom panel). Endogenous PLEKHG6 is detectable only after immunoprecipitation.

PLEKHG6-ΔCT (Figure 2C). Neither forms of PLEKHG6 were found to interact with the C-terminus of ezrin or full-length ezrin. These data indicate that the C-terminal region of PLEKHG6 is necessary and sufficient for its interaction with the N-terminal domain of ezrin. Moreover, they indicate that the binding site of PLEKHG6 on ezrin is masked due to the intramolecular

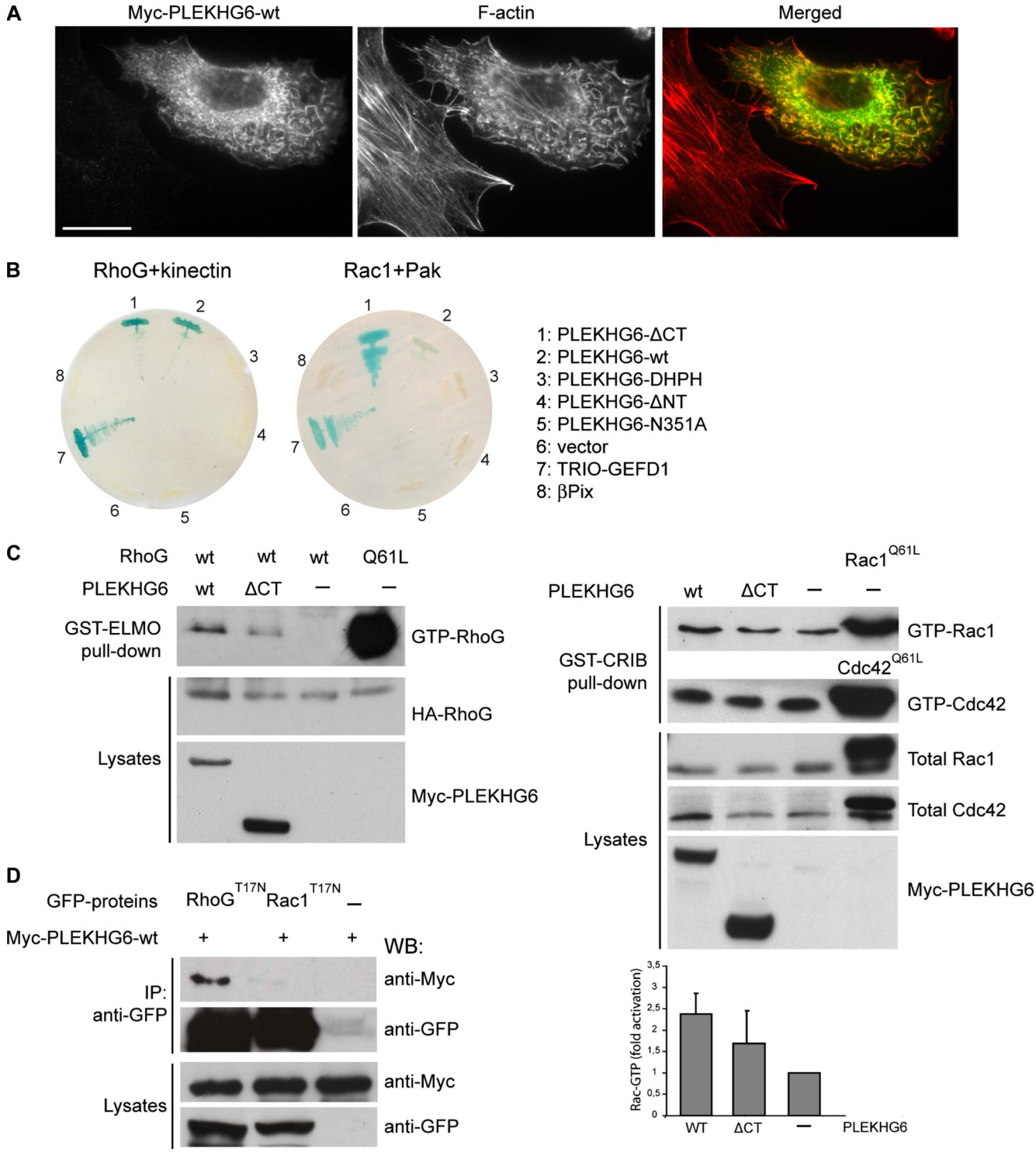

Figure 3. PLEKHG6 displays a guanine nucleotide exchange activity preferentially toward RhoG. (A) Morphogenic effects induced by PLEKHG6 in NIH3T3 cells. NIH3T3 cells transiently expressing Myc-tagged PLEKHG6 were stained with an anti-Myc antibody (green) and rhodamine-phalloidin (F-actin). PLEKHG6 induces dorsal microvilli and ruffles. A loss of actin stress fibers is observed in cells expressing PLEKHG6. Scale bar, 20 μm. (B) PLEKHG6 guanine nucleotide exchange activity in yeast. β-galactosidase activity reflecting the exchange activity of indicated PLEKHG6 forms toward RhoG (left panel) or Rac (right panel) is shown. PLEKHG6 displays an exchange activity toward RhoG and to a much lesser extent toward Rac. Trio-GEFD1 and βPix were used as positive and negative controls, respectively. The different PLEKHG6 proteins were produced at similar levels in yeast (data not shown). (C) PLEKHG6 stimulates GTP-loading on RhoG in vivo. Left panel: lysates of LLC-PK1 cells expressing HA-tagged RhoG and Myc-tagged PLEKHG6 were incubated with GST-ELMO immobilized on beads. GTP-RhoG (top) and total RhoG (middle) were detected with an anti-HA antibody. PLEKHG6 proteins were detected in the lysates with an anti-Myc antibody (bottom). As a control, lysates of cells expressing HA-RhoG^{Q61L} were incubated with GST-ELMO. Right panel: lysates of LLC-PK1 cells expressing PLEKHG6 proteins were incubated with GST-CRIB immobilized on beads. GTP-Rac1 or GTP-Cdc42 (top), and total Rac1 or Cdc42 (middle) was detected with anti-Rac1 and Cdc42 antibodies, respectively. PLEKHG6 were detected with an anti-Myc

interaction between the N- and C-terminal domains of ezrin. To confirm this observation, GST-ezrin-NT was incubated with lysates of cells expressing Myc-tagged PLEKHG6 in the absence or presence of the C-terminal domain of ezrin. As shown in Figure 2D, the interaction between Myc-PLEKHG6 and GST-ezrin-NT was inhibited by the addition of the C-terminal domain of ezrin. This indicates that PLEKHG6 interacts with ezrin only when the protein is in an open conformation. We also observed an interaction between PLEKHG6 and the N-terminal domain of radixin and a weak interaction with the N-terminal domain of moesin but not with the full-length proteins, indicating that as for ezrin the PLEKHG6 binding site on radixin and moesin is cryptic (data not shown).

The ability of PLEKHG6 to interact with ezrin was further confirmed in vivo by expression of Myc-tagged PLEKHG6 in LLC-PK1 cells stably transfected with the vector alone or with the cDNA coding for VSVG-tagged ezrin wt or T567D (T/D) followed by immunoprecipitation. The substitution of threonine 567 by aspartic acid in ERM proteins mimics the phosphorylation of threonine 567, which has been shown to prevent the N-/C-ERMAD association (Matsui *et al.*, 1998) and to increase the level of active ezrin in the cells (Gautreau *et al.*, 2000). We found that PLEKHG6 coimmunoprecipitates with ezrin T567D but not with ezrin wt (Figure 2E). Furthermore, ezrin T567D is coimmunoprecipitated with endogenous PLEKHG6 (Figure 2F). As expected, PLEKHG6-ΔCT failed to coimmunoprecipitate with ezrin T567D (Figure 2E). Altogether, these results show that PLEKHG6, through its C-terminal domain, interacts only with an active form of ezrin.

PLEKHG6 Displays Guanine Nucleotide Exchange Activity Preferentially on RhoG

To establish that the identified PLEKHG6 had the capacity to activate Rho GTPases, we analyzed the morphological changes induced by PLEKHG6 in NIH3T3 cells. Transient expression of Myc-tagged PLEKHG6 promoted microvilli formation and membrane ruffles on the dorsal surface of the cells as well as a loss of stress fibers (Figure 3A). The effects induced by PLEKHG6, membrane ruffling, and loss of stress fibers suggested that the morphological changes observed might result from the activation of Rho GTPases of the Rac subfamily, including Rac1 and RhoG (Ridley *et al.*, 1992; Gauthier-Rouviere *et al.*, 1998). We therefore examined the ability of PLEKHG6 to activate RhoG and Rac1 in the yeast exchange assay (De Toledo *et al.*, 2000). In this assay, yeast expressing wild-type RhoG or Rac1 and their respective effectors, kinectin or Pak, were transformed with the cDNA coding for PLEKHG6-wt or a mutant form (PLEKHG6-N351A, PLEKHG6-ΔCT, PLEKHG6-ΔNT, PLEKHG6-DHPH). The activation of the Rho GTPases by the GEFs leads to their interaction with their effectors and this interaction is monitored by the β-galactosidase activity. As shown in Figure 3B, wild-type PLEKHG6 activated RhoG to the same extent as the exchange factor Trio-GEFD1, which was used as positive control. PLEKHG6-N351A containing a single amino acid substitution of the highly conserved Asn^{351} in the DH domain had no exchange activity and therefore represents a catalytically dead form of PLEKHG6 (Whitehead *et al.*, 1997; Aghazadeh *et al.*, 1998; Debreceni *et al.*, 2004). PLEKHG6 lacking the ezrin binding site (PLEKHG6-ΔCT) exhibited an exchange activity toward RhoG, similar to that of the full-length protein (Figure 3B, left panel). However, neither the DH/PH tandem nor PLEKHG6-ΔNT showed an exchange activity toward RhoG. No exchange activity for the DH/PH domains was observed in an in vitro assay (data not shown). Altogether this indicates that, whereas the C-terminal region of PLEKHG6 is dispensable for the guanine nucleotide exchange activity, the N-terminal region of PLEKHG6 is required. An exchange activity of PLEKHG6 was also observed toward Rac1 although to a much lesser extent than that of Trio-GEFD1 toward Rac1 (Figure 3B, right panel). However, the β-galactosidase activity induced by PLEKHG6-ΔCT was stronger than that of PLEKHG6. Next, we measured the exchange activity of Myc-tagged PLEKHG6 by pulldown using GST-ELMO and GST-CRIB domains of Pak1 to evaluate the level of GTP-bound RhoG, Rac1, and Cdc42, respectively. Because endogenous RhoG cannot be detected with the available antibodies a low level of HA-RhoG was expressed in cells. Transient expression of PLEKHG6 increased significantly the amount of GTP-bound RhoG (Figure 3C, left panel). PLEKHG6-ΔCT was still able to promote GTP-loading of RhoG, although to a lower extent than PLEKHG6-wt (Figure 3C, left panel). A low increase (2.3-fold) in GTP-bound Rac1 was observed upon expression of PLEKHG6-wt, but unlike what was observed in the yeast exchange assay, PLEKHG6-ΔCT only slightly increased the level of GTP-bound Rac1 (1.6-fold; Figure 3C, right panels). No detectable increase in the amount of GTP-bound Cdc42 was detected upon expression of either PLEKHG6-wt or PLEKHG6-ΔCT (Figure 3C, right panel). Together, these results indicate that PLEKHG6 has an exchange activity toward RhoG and to a much lesser degree toward Rac1.

Next, we examined the ability of PLEKHG6 to associate with the negative forms of RhoG and Rac1 containing the point mutation T17N. This mutation is thought to disrupt the binding of guanine nucleotides, generating nucleotide-free GTPases that have a high binding affinity for the GEFs (Feig and Cooper, 1988a,b). Myc-PLEKHG6-wt was expressed in 293T cells together with GFP-$RhoG^{T17N}$ or GFP-$Rac1^{T17N}$, and immunoprecipitation with an anti-GFP antibody was performed (Figure 3D). PLEKHG6-wt coimmunoprecipitated with $RhoG^{T17N}$, whereas only a very weak band was detected with $Rac1^{T17N}$. This indicates that RhoG may be the main target of PLEKHG6.

Ezrin Determines the Subcellular Localization of PLEKHG6

We next analyzed the morphological changes triggered by PLEKHG6 in LLC-PK1 epithelial cells because in these cells ezrin plays an important role in the organization of the apical brush border microvilli (Gautreau *et al.*, 2000). Because endogenous PLEKHG6 could not be detected by immunofluorescence (data not shown), we transiently expressed PLEKHG6 in LLC-PK1 cells. Myc-PLEKHG6-wt induced actin-rich apical ruffles and microvilli as shown by rhodamine-phalloidin staining (Figure 4A, top panel). Colocalization of ezrin and Myc-PLEKHG6-wt was observed in these structures (Figure 4B, top panel). The formation of the

Figure 3 (cont). antibody (bottom). As a control, lysates of cells expressing Myc-$Rac1^{Q61L}$ or Myc-$Cdc42^{Q61L}$ were incubated with GST-CRIB. Densitometric quantification: Rac activity was calculated from the amount of GTP-bound Rac1 normalized to the amount of total Rac in cell lysates. An arbitrary unit of 1 was given for Rac1 activity in cells that do not produce PLEKHG6. Rac activity is induced 2.3-fold in cells producing PLEKHG6-wt and 1.6-fold in cells producing PLEKHG6-ΔCT. Error bars, the SD between three independent experiments. (D) RhoG is the main target of PLEKHG6 in vivo. 293T cells were cotransfected with plasmids encoding Myc-PLEKHG6 and GFP-$RhoG^{TN17}$ or GFP-Rac^{T17N}. Cell lysates were immunoprecipitated with an anti-GFP antibody and immunoblotting was performed with an anti-Myc antibody to detect associated PLEKHG6 proteins. Western blots were performed on cell lysates with the indicated antibodies (bottom panel).

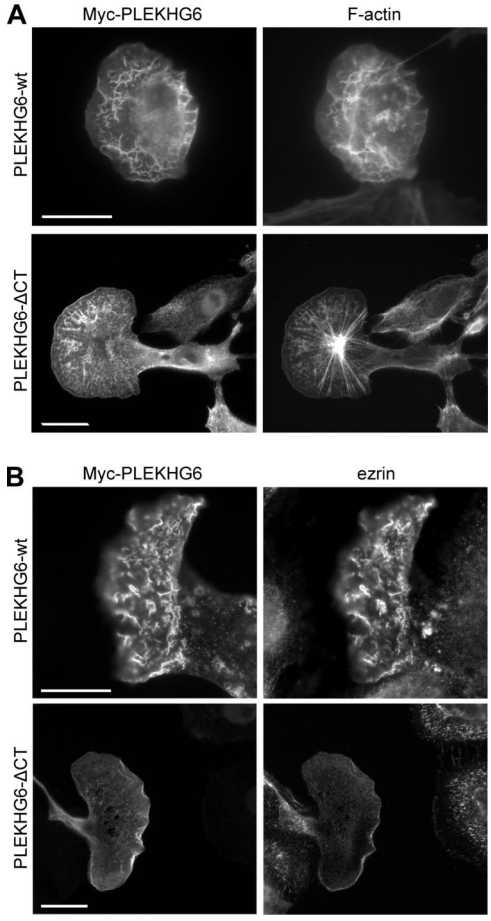

Figure 4. PLEKHG6 induces apical microvilli and ruffles in epithelial cells. (A) LLC-PK1 cells transfected with Myc-tagged PLEKHG6-wt or PLEKHG6-ΔCT were immunostained with a Myc antibody. F-actin was stained with rhodamine-phalloidin. Scale bar, 20 μm. (B) Double immunofluorescence was performed with an anti-Myc and an anti-ezrin antibody. Endogenous ezrin colocalizes with Myc-PLEKHG6 in the apical microvilli and ruffles. PLEKHG6-ΔCT lacking the ezrin binding site induces extensive lamellipodia. Scale bar, 20 μm.

apical actin-rich structures was not detected in cells expressing Myc-PLEKHG6-ΔCT, which does not interact with ezrin (Figure 4A, bottom panel). Instead, the cells were flattened and formed extensive lamellipodia (Figure 4, A and B, bottom panels). We also observed in these cells actin-rich patches probably corresponding to actin nucleation sites (Figure 4A, bottom panel). Altogether, these observations indicate that the recruitment of PLEKHG6 by ezrin controls actin cytoskeleton organization at the apical surface of the cells. Consistent with this, we found that the catalytically dead form Myc-PLEKHG6-N351A, which still interacts with ezrin (data not shown), colocalized with ezrin in the microvilli (see inset) and did not induce changes in cell morphology (Figure 5A, top panel). In contrast Myc-PLEKHG6-N351A-ΔCT showed a diffuse cytoplasmic staining and had no effect on cell morphology as these cells bear regular microvilli at the apical surface (Figure 5A, bottom panel). We did not observe any morphological changes in cells expressing the DH/PH domains (data not shown), thus confirming that the DH/PH domains alone display no exchange activity.

Based on our results that showed a specificity of PLEKHG6 toward RhoG, we hypothesized that inhibiting RhoG signaling could block the morphogenic effects induced by PLEKHG6. Thus we coexpressed Myc-PLEKHG6-wt together with negative mutants of RhoG in LLC-PK1 cells. Although cells expressing Myc-PLEKHG6-wt alone displayed membrane ruffling at their apical surface (Figure 4, A and B, top panels), cells coexpressing Myc-PLEKHG6-wt and GFP-RhoG^{T17N} or GFP-RhoG^{F37A} had a regular shape and displayed well-organized apical microvilli in which PLEKHG6 was present (Figure 5B). We could also observe a small pool of dominant negative RhoG in the microvilli when PLEKHG6 was coexpressed (Figure 5B). These results further indicate that PLEKHG6 induces its morphogenic effects at the apical surface of the cells through the activation of RhoG.

PLEKHG6 Forms a Ternary Complex with Ezrin and RhoG

Our results suggested that ezrin/PLEKHG6 interaction is important for RhoG-mediated signaling pathways at the apical surface of the cells. Therefore, we determined whether ezrin and PLEKHG6 could form a ternary complex with RhoG. We transiently transfected 293T cells with GFP-RhoG^{T17N} and VSVG-ezrin-Δ29, which represents an open form of ezrin, in the presence or absence of Myc-PLEKHG6. As shown in Figure 6, a ternary complex was observed in the presence of wild-type PLEKHG6 but not PLEKHG6-ΔCT. In the absence of PLEKHG6 we detected a very weak association of GFP-RhoG^{T17N} with VSVG-ezrin-Δ29. This interaction might be mediated by the endogenous PLEKHG6 or, alternatively, by a RhoGDI, which has been shown to interact with ezrin (Takahashi *et al.*, 1997). Although equal amounts of total DNA were used in all transfections, we repeatedly found that the amount of GFP-RhoG^{T17N} expressed in cells producing PLEKHG6-ΔCT was very low, suggesting that RhoG^{T17N} is less stable in presence of this mutant. Altogether these data indicated that a ternary complex between ezrin, PLEKHG6, and RhoG could form, with PLEKHG6 bridging RhoG^{T17N} and ezrin.

PLEKHG6 Interacts with the RhoG Effector ELMO

Because an interaction between ERM proteins and the effector of RhoG ELMO has been described (Grimsley *et al.*, 2006), we analyzed the potential molecular association between the components of the RhoG pathway. We coexpressed in 293T cells GFP-ELMO with an open form of ezrin VSVG-ezrin-Δ29 and Myc-tagged PLEKHG6-wt or PLEKHG6-ΔCT, and we performed immunoprecipitations with either anti-GFP or -VSVG antibodies. Interestingly, we found that ELMO immunoprecipitated PLEKHG6 and ezrin-Δ29 (Figure 7A, top panel, lane 2). A complex was also observed with PLEKHG6-ΔCT that does not bind to ezrin, indicating that the interaction between PLEKHG6 and ELMO was not mediated by ezrin (Figure 7A, top panel, lane 3). These results indicate that PLEKHG6 and ezrin binding sites on ELMO are distinct, allowing the formation of a ternary complex. When immunoprecipitation of VSVG-ezrin was performed, we confirmed that a complex between ezrin-Δ29, ELMO and PLEKHG6-wt could occur (Figure 7A, middle panel, lane 2). In the presence of PLEKHG6-ΔCT only ELMO was immunoprecipitated with VSVG-ezrin-Δ29 (Figure 7A, middle panel, lane 3). The amount of ELMO associated with ezrin-Δ29 in the presence of PLEKHG6-ΔCT was very low compared with PLEKHG6-wt, suggesting that PLEKHG6 may influence the interaction between ELMO and ezrin. To further confirm the interaction between ELMO and PLEKHG6, GST-ELMO immobilized on beads was in-

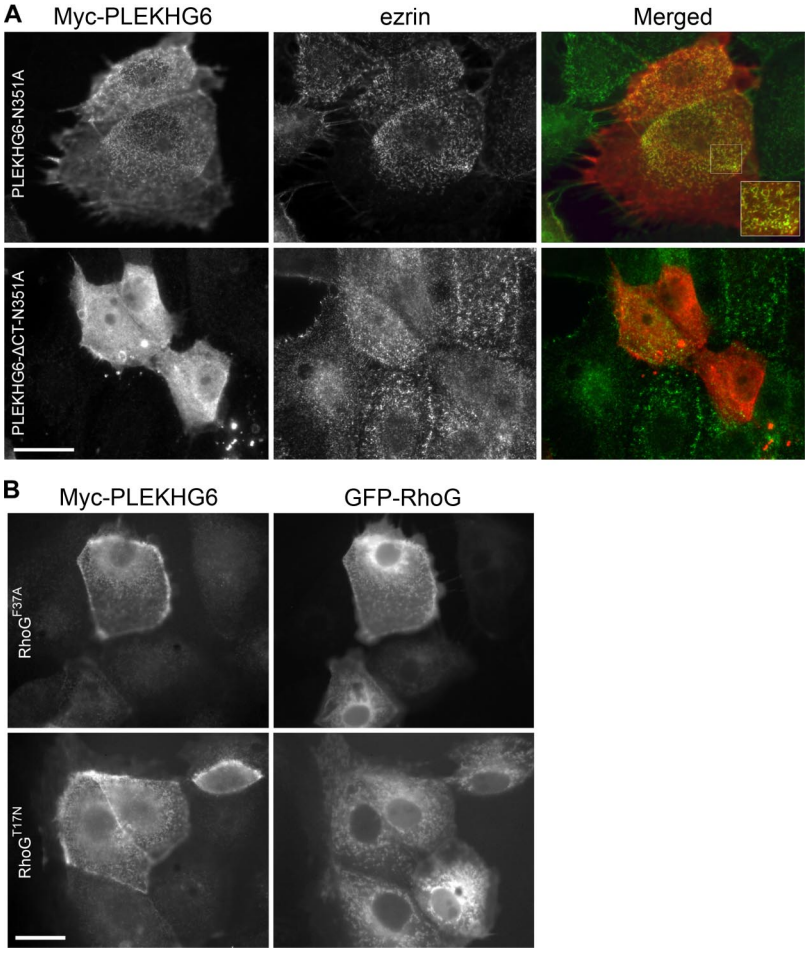

Figure 5. Ezrin targets PLEKHG6 to the apical surface of epithelial cells. (A) LLC-PK1 cells expressing Myc-tagged PLEKHG6-N351A or PLEKHG6-N351A-ΔCT were immunostained with a monoclonal anti-Myc antibody (red) and a polyclonal anti-ezrin antibody (green). PLEKHG6-N351A but not PLEKHG6-N351A-ΔCT colocalizes with ezrin to the apical microvilli (merged and inset). (B) PLEKHG6-induced morphogenic effects are impaired in presence of $RhoG^{T17N}$ or $RhoG^{F37A}$. Immunofluorescence of LLC-PK1 cells expressing Myc-tagged PLEKHG6-wt and GFP-$RhoG^{T17N}$ or GFP-$RhoG^{F37A}$ was performed with an anti-Myc antibody. Scale bar, 20 μm.

cubated with lysates from 293T cells expressing different Myc-tagged forms of PLEKHG6. We found that GST-ELMO pulled down PLEKHG6-wt as well as PLEKHG6-ΔCT, confirming that ELMO binding site on PLEKHG6 is distinct from that of ezrin (Figure 7B). We also observed that GST-ELMO binds to PLEKHG6-ΔNT suggesting that the ELMO binding site on PLEKHG6 is likely to be located within their DH/PH domains (Figure 7B). Altogether these results indicate that ezrin is present in distinct complexes, because it interacts with PLEKHG6 or ELMO, it also forms a ternary complex with these two proteins. Moreover we show that PLEKHG6 and ELMO can interact together independently of ezrin.

Ezrin and PLEKHG6 Are Required for EGF-stimulated Macropinocytosis in A431 Cells

Actin cytoskeleton rearrangements resulting in formation of membrane ruffles are known to promote macropinocytosis. Because PLEKHG6 induced apical ruffles through its interaction with ezrin, we examined whether these two proteins contributed to macropinocytosis in the human epidermoïd carcinoma cells, A431. We analyzed the consequence of PLEKHG6 or ezrin depletion on macropinocytosis. The uptake of TRITC-dextran (TRDx) was scored in cells expressing the shRNAs for either PLEKHG6 or ezrin. The efficiency of shRNAs in the inhibition of PLEKHG6 expression was tested on the overexpressed protein or at the level of mRNA for the endogenous protein, because endogenous PLEKHG6 can neither be detected by Western blot nor by immunoflu-

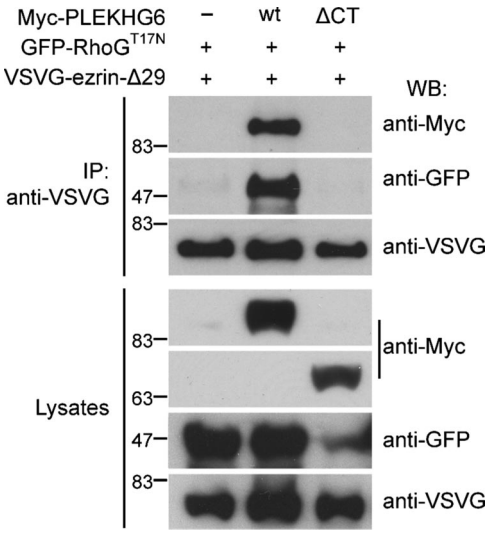

Figure 6. Ezrin forms a ternary complex with PLEKHG6 and RhoG. 293T cells were cotransfected with plasmids encoding Myc-PLEKHG6-wt or Myc-PLEKHG6-ΔCT, GFP-$RhoG^{T17N}$ and VSVG-ezrin-Δ29 as indicated. Immunoprecipitations were performed with an anti-VSVG antibody followed by immunoblotting with anti-Myc and anti-GFP antibodies. Western blots were performed on cell lysates with the indicated antibodies (bottom panel).

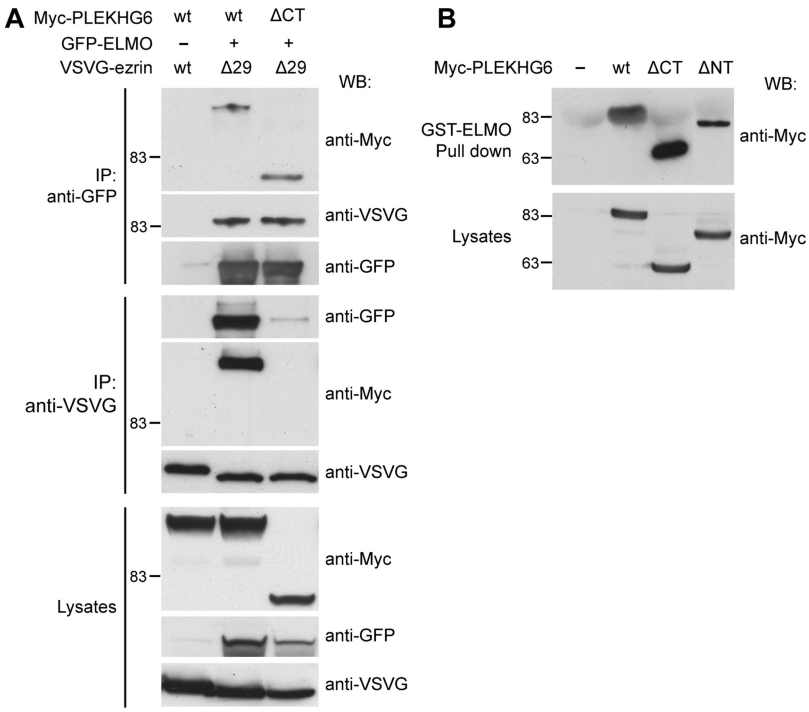

Figure 7. Ezrin and PLEKHG6 interact with ELMO. (A) PLEKHG6, ezrin, and ELMO form a ternary complex. 293T cells were cotransfected with the indicated plasmids. Immunoprecipitations were performed with anti-GFP (top panel) or anti-VSVG (middle panel) antibodies. Western blots on the immunoprecipitated proteins and cell lysates were performed with the indicated antibodies. (B) PLEKHG6 interacts with ELMO. Lysates of 293T cells producing various Myc-tagged forms of PLEKHG6 were incubated with GST-ELMO. Proteins were detected by Western blot with an anti-Myc antibody.

orescence. As shown in Figure 8A, PLEKHG6 shRNA 1 and 2 led to an efficient down-regulation of PLEKHG6 both at the protein (top panel) and mRNA (bottom panel) levels and were used in subsequent experiments. Expression of two different shRNAs targeting ezrin (psiEz1, psiEz2) led to efficient knockdown because in shRNA-expressing cells that were also GFP positive no ezrin labeling was observed by immunofluorescence (Figure 8B, bottom panel). By Western blot, the failure to knock down ezrin completely at the protein levels, as observed by immunofluorescence, reflects a transfection efficiency of 60% (Figure 8B, top panel). However, we observed that inhibition of ezrin expression prevented the formation of PLEKHG6-induced dorsal ruffles. As shown in Figure 8C, A431 cells producing scramble shRNA and PLEKHG6 displayed dorsal membrane ruffles, whereas A431 cells producing ezrin shRNA and PLEKHG6 were more flat and exhibited small microvilli but no membrane ruffles. This indicated that the ability of PLEKHG6 to induce the formation of dorsal ruffles is directly linked to its binding to ezrin. We next measured the macropinocytosis of TRDx in A431 cells stimulated with EGF, which increases their pinocytotic activity (Haigler *et al.*, 1979). The uptake of TRITC-dextran was measured in cells expressing scramble, PLEKHG6, or ezrin shRNAs that were also GFP positive (Figure 8D). We observed a striking decrease in TRITC-dextran uptake in cells expressing PLEKHG6 (~23%) or ezrin shRNAs (~27%) compared with cells expressing scrambled shRNAs (~65%; Figure 8D). Interestingly, the inhibition of dextran uptake was similar in cells knocked down for either PLEKHG6 or ezrin, suggesting that these proteins are both required for macropinocytosis.

DISCUSSION

In this article we describe the identification and characterization of a novel GEF for RhoG, PLEKHG6. We find that the interaction of PLEKHG6 with ezrin acting as a membrane-cytoskeleton linker is required for its localization to the apical surface of the cells where it induces morphological changes. We demonstrate that both PLEKHG6 and ezrin are required for membrane ruffles-mediated macropinocytosis. Furthermore, we provide evidence that ezrin, by recruiting components of the RhoG pathway in a close proximity, allows a tight regulation of RhoG activation at the apical surface of epithelial cells.

Phylogenetic trees of human GEFs indicate that PLEKHG6 together with GEF720 form a phylogenetic subgroup (Schmidt and Hall, 2002; Rossman *et al.*, 2005). These two proteins share significant homologies in their DH/PH domains with the Dbl-related proteins from *D. melanogaster* (CG7323) and *C. elegans* (T08H4.1). Thus CG7323 and T08H4.1 may represent the invertebrate homologues of PLEKHG6 and GEF720. Because neither of these proteins has been characterized so far it is not known if they are functionally related.

Here, we demonstrate by different approaches that PLEKHG6 displays an exchange activity primarily toward RhoG although a very low exchange activity of PLEKHG6 toward Rac1 was observed. Consistent with these data we found a strong association of PLEKHG6 with nucleotide-free RhoG and a very weak association with nucleotide-free Rac1. Other GEFs for RhoG have been described, such as TrioGEF1, Kal-GEF1, and SGEF (Blangy *et al.*, 2000; May *et al.*, 2002; Ellerbroek *et al.*, 2004), which in addition to their preferential activity toward RhoG, can also activate another Rho GTPase. Thus Kal-GEF1 and TrioGEF1 activates Rac1, whereas SGEF activates Cdc42.

We have observed an unusual regulation of the exchange activity of PLEKHG6. Unlike what is observed with most GEFs, we found that the DH/PH tandem of PLEKHG6 has no exchange activity either in vitro or in the yeast exchange assay or in cells. Furthermore, we observed that removal of the N-terminal domain leads to an inactive protein. For other GEFs, however, it has been reported that deletion of the N-terminal domain leads to constitutive activation by the relief of an intramolecular autoinhibition (Schmidt and

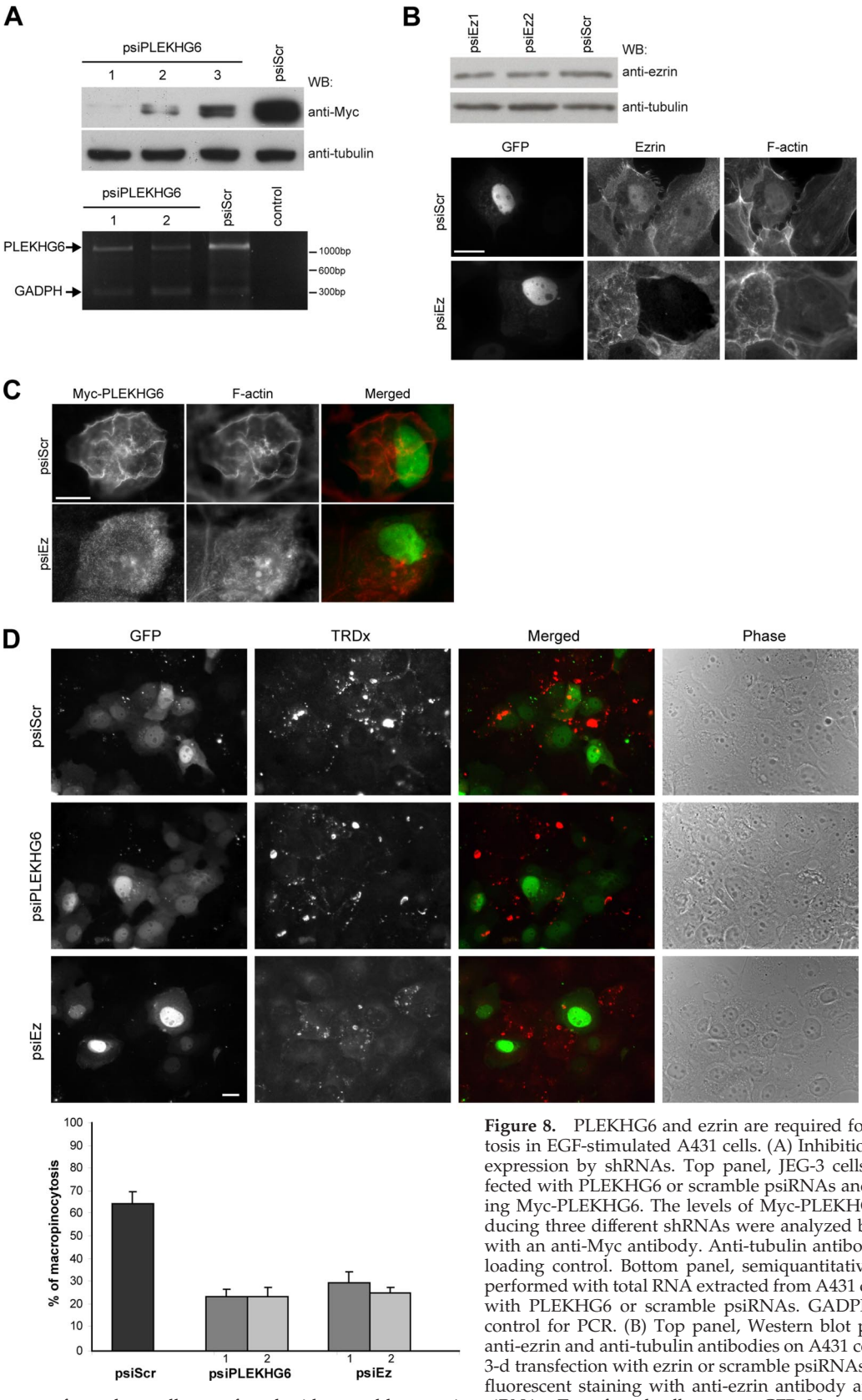

Figure 8. PLEKHG6 and ezrin are required for macropinocytosis in EGF-stimulated A431 cells. (A) Inhibition of PLEKHG6 expression by shRNAs. Top panel, JEG-3 cells were cotransfected with PLEKHG6 or scramble psiRNAs and cDNA encoding Myc-PLEKHG6. The levels of Myc-PLEKHG6 in cells producing three different shRNAs were analyzed by Western blot with an anti-Myc antibody. Anti-tubulin antibody was used as loading control. Bottom panel, semiquantitative RT-PCR was performed with total RNA extracted from A431 cells transfected with PLEKHG6 or scramble psiRNAs. GADPH was used as control for PCR. (B) Top panel, Western blot performed with anti-ezrin and anti-tubulin antibodies on A431 cell extracts after 3-d transfection with ezrin or scramble psiRNAs. Bottom panel, fluorescent staining with anti-ezrin antibody and Alexa Fluor 350 phalloidin was performed on cells transfected with scramble or ezrin psiRNAs. Transfected cells express GFP. No ezrin staining was detected in cells transfected with either psiEz1 or psiEz2 (not shown). (C) Ezrin knockdown inhibits PLEKHG6-induced dorsal ruffles. After 2-d transfection with ezrin or scramble psiRNAs, A431 cells were transfected with the plasmid encoding Myc-PLEKHG6-wt. Fluorescent staining was performed with anti-myc antibody and Alexa Fluor 350 phalloidin. The merged image represents F-actin staining in red, and

Hall, 2002). This suggests that other mechanisms are involved in the activation of PLEKHG6. For example, conformational changes may be triggered by the interaction of proteins with the amino-terminal domain of PLEKHG6, thus controlling its activity. In contrast, we found that the ezrin-binding site in the C-terminus of PLEKHG6 is dispensable for its exchange activity, indicating that ezrin is not directly implicated in the regulation of PLEKHG6 activity.

Instead, our results demonstrate that the interaction between ezrin and PLEKHG6 is important for the localization of PLEKHG6 in a specific epithelial cell compartment. This interaction is regulated because it can only occur when ezrin is in an open conformation acting as a membrane-cytoskeleton linker. In epithelial cells, the pool of ezrin that is associated with the cortical actin cytoskeleton is mainly present at the apical membrane domains in structures such as microvilli. Indeed, we observed that both PLEKHG6 and PLEKHG6-N351A colocalize with ezrin at the apical pole of the cells, whereas mutants of PLEKHG6 lacking the C-terminal ezrin-binding site do not.

Consistent with this specific localization, PLEKHG6 induces the remodeling of the apical actin structures in epithelial cells with formation of apical ruffles and microvilli triggered by the activation of RhoG. In support of this, dominant negative mutants of RhoG efficiently inhibit the specific PLEKHG6-induced morphogenic effects. Interestingly, in cells knocked down for ezrin, PLEKHG6 does not induce dorsal ruffles but lamellipodia, as does PLEKHG6-ΔCT, which fails to interact with ezrin. These observations suggest that when the interaction ezrin/PLEKHG6 is abolished, PLEKHG6 or PLEKHG6-ΔCT may elicit actin cytoskeleton rearrangements through different effectors depending on which compartment RhoG is activated.

In our model we have observed distinct complexes involving components of the RhoG pathway. A ternary complex between ezrin, PLEKHG6 and RhoG was found, indicating that RhoG is recruited to the apical compartment by PLEKHG6 when associated with ezrin. This was supported by immunofluorescence data showing a pool of RhoG in the microvilli. In agreement with a previous report describing an interaction between ELMO and ERM proteins (Grimsley *et al.*, 2006), we found that ezrin interacts with ELMO. Furthermore, we observed a ternary complex between ezrin, PLEKHG6, and ELMO, suggesting that ezrin recruits upstream and downstream regulators of RhoG. Interestingly, we also found an interaction between PLEKHG6 and ELMO that was not mediated by ezrin. These findings suggest that PLEKHG6 may interact directly with the RhoG effector ELMO. We cannot, however, exclude that the interaction between PLEKHG6 and ELMO occurs through RhoG. The interaction of GEFs with Rho GTPases effectors has already been reported. For example, the interaction of Dbl with Pak has been shown to have a positive feedback on the Dbl exchange activity toward Cdc42 (Wang *et al.*, 2004). Other studies indicate that GEFs can also interact with and activate the effector in an exchange activity–independent manner, as shown for Kal-GEF1, and αPix that can interact with and activate Pak (Daniels *et al.*, 1999; Schiller *et al.*, 2005). Therefore, the interaction of PLEKHG6 with ELMO may serve to activate specific RhoG downstream pathways. Alternatively, a regulatory feedback loop might exist, whereby ELMO could regulate the exchange activity of PLEKHG6. Altogether our data indicate that ezrin coordinates the association between the upstream and downstream regulators of RhoG pathways in a specific subcellular compartment allowing the local activation of RhoG.

We demonstrate here that the formation of dorsal ruffles triggered by PLEKHG6, is important for efficient macropinocytosis in A431 cells. In this process, ezrin is required for the formation of dorsal ruffles by PLEKHG6 and therefore for RhoG activation in a specific cellular compartment. Moreover we show that the interaction between ezrin and PLEKHG6 is necessary for macropinocytosis. Indeed, downregulation of either PLEKHG6 or ezrin inhibits to the same extent the dextran uptake in EGF-stimulated A431 cells. SGEF, an exchange factor for RhoG has been shown to stimulate macropinocytosis in NIH3T3 cells (Ellerbroek *et al.*, 2004) and to mediate *Salmonella* entry into cells through the reorganization of the actin cytoskeleton (Patel and Galan, 2006). This suggests that activation of RhoG may participate not only to cytoskeleton reorganization but also to processes involved in internalization of molecules. Interestingly, the highest level of PLEKHG6 mRNA is observed in placenta, a tissue in which ezrin is abundant (West *et al.*, 1989). Placental microvilli are very dynamic structures actively involved in nutrient exchange. Therefore, the interaction between ezrin and PLEKHG6 described here could play an important role in functions associated with the placental microvilli.

Figure 8 (cont). the GFP is indicative of cells transfected with the psiRNA. (D) Fluorescent-dextran uptake in EGF-treated A431 cells. Three days after transfection of A431 cells with psiRNAs, the uptake of TRITC-dextran (TRDx) was performed in presence of EGF. Dextran uptake was scored in transfected cells producing GFP. For each psiRNA and in three independent experiments, at least 50 cells expressing GFP were examined for dextran uptake. As shown in the bar diagram, TRITC-dextran uptake was observed in ~65% of cells producing scramble shRNA, whereas only ~23 and 27% of cells producing PLEKHG6 and ezrin shRNAs, respectively, were positive. Error bars, SD. Scale bar, 20 μm.

ACKNOWLEDGMENTS

The authors thank Dr. L. Daviet and all Hybrigenics staff for yeast two-hybrid analysis. We thank Drs. P. Chavrier, R. Zaarour, C. Recchi, and J. Sillibourne for critical reading of the manuscript and for helpful suggestions. We are grateful to Drs. A. Hall, P. Fort, P. Lowe, J. Camonis, and K. Ravichandran and the National Institute of Technology and Evaluation (Japan) for the gift of plasmids. This work was supported by grants from GenHomme network Grant (02490-6088) to Hybrigenics and Institut Curie, Association pour la Recherche contre le Cancer (ARC-MA-3267), Agence Nationale de la Recherche (ANR 05BLAN033001) and Fondation pour la Recherche Médicale (FRM) to M.A. R.D'A. is a recipient of fellowships from GenHomme and Institut Curie.

REFERENCES

Aghazadeh, B., Zhu, K., Kubiseski, T. J., Liu, G. A., Pawson, T., Zheng, Y., and Rosen, M. K. (1998). Structure and mutagenesis of the Dbl homology domain. Nat. Struct. Biol. *5*, 1098–1107.

Barret, C., Roy, C., Montcourrier, P., Mangeat, P., and Niggli, V. (2000). Mutagenesis of the phosphatidylinositol 4,5-biphosphate (PIP2) binding site in the NH2-terminal domain of ezrin correlates with its altered cellular distribution. J. Cell Biol. *151*, 1067–1079.

Berryman, M., Franck, Z., and Bretscher, A. (1993). Ezrin is concentrated in the apical microvilli of a wide variety of epithelial cells whereas moesin is found primarily in endothelial cells. J. Cell Sci. *105*, 1025–1043.

Berryman, M., Gary, R., and Bretscher, A. (1995). Ezrin oligomers are major cytoskeletal components of placental microvilli: a proposal for their involvement in cortical morphogenesis. J. Cell Biol. *131*, 1231–1242.

Blangy, A., Vignal, E., Schmidt, S., Debant, A., Gauthier-Rouviere, C., and Fort, P. (2000). TrioGEF1 controls Rac- and Cdc42-dependent cell structures through the direct activation of rhoG. J. Cell Sci. *113*(Pt 4), 729–739.

Bonilha, V. L., Rayborn, M. E., Saotome, I., McClatchey, A. I., and Hollyfield, J. G. (2006). Microvilli defects in retinas of ezrin knockout mice. Exp. Eye Res. *82*, 720–729.

Bretscher, A., Edwards, K., and Fehon, R. G. (2002). ERM proteins and merlin: integrators at the cell cortex. Nat. Rev. Mol. Cell Biol. *3*, 586–599.

Daniels, R. H., Zenke, F. T., and Bokoch, G. M. (1999). alphaPix stimulates p21-activated kinase activity through exchange factor-dependent and -independent mechanisms. J. Biol. Chem. *274*, 6047–6050.

De Toledo, M., Colombo, K., Nagase, T., Ohara, O., Fort, P., and Blangy, A. (2000). The yeast exchange assay, a new complementary method to screen for Dbl-like protein specificity: identification of a novel RhoA exchange factor. FEBS Lett. *480*, 287–292.

deBakker, C. D. *et al.* (2004). Phagocytosis of apoptotic cells is regulated by a UNC-73/TRIO-MIG-2/RhoG signaling module and armadillo repeats of CED-12/ELMO. Curr. Biol. *14*, 2208–2216.

Debreceni, B., Gao, Y., Guo, F., Zhu, K., Jia, B., and Zheng, Y. (2004). Mechanisms of guanine nucleotide exchange and Rac-mediated signaling revealed by a dominant negative trio mutant. J. Biol. Chem. *279*, 3777–3786.

Ellerbroek, S. M., Wennerberg, K., Arthur, W. T., Dunty, J. M., Bowman, D. R., DeMali, K. A., Der, C., and Burridge, K. (2004). SGEF, a RhoG guanine nucleotide exchange factor that stimulates macropinocytosis. Mol. Biol. Cell *15*, 3309–3319.

Estrach, S., Schmidt, S., Diriong, S., Penna, A., Blangy, A., Fort, P., and Debant, A. (2002). The human Rho-GEF trio and its target GTPase RhoG are involved in the NGF pathway, leading to neurite outgrowth. Curr. Biol. *12*, 307–312.

Faure, S., Salazar-Fontana, L. I., Semichon, M., Tybulewicz, V. L., Bismuth, G., Trautmann, A., Germain, R. N., and Delon, J. (2004). ERM proteins regulate cytoskeleton relaxation promoting T cell-APC conjugation. Nat. Immunol. *5*, 272–279.

Feig, L. A., and Cooper, G. M. (1988a). Inhibition of NIH 3T3 cell proliferation by a mutant ras protein with preferential affinity for GDP. Mol. Cell. Biol. *8*, 3235–3243.

Feig, L. A., and Cooper, G. M. (1988b). Relationship among guanine nucleotide exchange, GTP hydrolysis, and transforming potential of mutated ras proteins. Mol. Cell. Biol. *8*, 2472–2478.

Fiévet, B., Louvard, D., and Arpin, M. (2007). ERM proteins in epithelial cell organization and functions. Biochim. Biophys. Acta *1773*, 653–660.

Fiévet, B. T., Gautreau, A., Roy, C., Del Maestro, L., Mangeat, P., Louvard, D., and Arpin, M. (2004). Phosphoinositide binding and phosphorylation act sequentially in the activation mechanism of ezrin. J. Cell Biol. *164*, 653–659.

Formstecher, E. *et al.* (2005). Protein interaction mapping: a *Drosophila* case study. Genome Res. *15*, 376–384.

Gary, R., and Bretscher, A. (1995). Ezrin self-association involves binding of an N-terminal domain to a normally masked C-terminal domain that includes the F-actin binding site. Mol. Biol. Cell *6*, 1061–1075.

Gauthier-Rouviere, C., Vignal, E., Meriane, M., Roux, P., Montcourier, P., and Fort, P. (1998). RhoG GTPase controls a pathway that independently activates Rac1 and Cdc42Hs. Mol. Biol. Cell *9*, 1379–1394.

Gautreau, A., Louvard, D., and Arpin, M. (2000). Morphogenic effects of ezrin require a phosphorylation-induced transition from oligomers to monomers at the plasma membrane. J. Cell Biol. *150*, 193–203.

Grimsley, C. M., Kinchen, J. M., Tosello-Trampont, A. C., Brugnera, E., Haney, L. B., Lu, M., Chen, Q., Klingele, D., Hengartner, M. O., and Ravichandran, K. S. (2004). Dock180 and ELMO1 proteins cooperate to promote evolutionarily conserved Rac-dependent cell migration. J. Biol. Chem. *279*, 6087–6097.

Grimsley, C. M., Lu, M., Haney, L. B., Kinchen, J. M., and Ravichandran, K. S. (2006). Characterization of a novel interaction between ELMO1 and ERM proteins. J. Biol. Chem. *281*, 5928–5937.

Gumienny, T. L. *et al.* (2001). CED-12/ELMO, a novel member of the CrkII/Dock180/Rac pathway, is required for phagocytosis and cell migration. Cell *107*, 27–41.

Haigler, H. T., McKanna, J. A., and Cohen, S. (1979). Rapid stimulation of pinocytosis in human carcinoma cells A-431 by epidermal growth factor. J. Cell Biol. *83*, 82–90.

Hirao, M., Sato, N., Kondo, T., Yonemura, S., Monden, M., Sasaki, T., Takai, Y., Tsukita, S., and Tsukita, S. (1996). Regulation mechanism of ERM (Ezrin/Radixin/Moesin) protein/plasma membrane association: possible involvement of phosphatidylinositol turnover and rho-dependent signaling pathway. J. Cell Biol. *135*, 37–51.

Katoh, H., Hiramoto, K., and Negishi, M. (2006). Activation of Rac1 by RhoG regulates cell migration. J. Cell Sci. *119*, 56–65.

Katoh, H., and Negishi, M. (2003). RhoG activates Rac1 by direct interaction with the Dock180-binding protein Elmo. Nature *424*, 461–464.

Katoh, H., Yasui, H., Yamaguchi, Y., Aoki, J., Fujita, H., Mori, K., and Negishi, M. (2000). Small GTPase RhoG is a key regulator for neurite outgrowth in PC12 cells. Mol. Cell Biol. *20*, 7378–7387.

Kreis, T. E. (1986). Microinjected antibodies against the cytoplasmic domain of vesicular stomatitis virus glycoprotein block its transport to the cell surface. EMBO J. *5*, 931–941.

Lee, J. H., Katakai, T., Hara, T., Gonda, H., Sugai, M., and Shimizu, A. (2004). Roles of p-ERM and Rho-ROCK signaling in lymphocyte polarity and uropod formation. J. Cell Biol. *167*, 327–337.

Mackay, D.J.G., Esch, F., Furthmayr, H., and Hall, A. (1997). Rho- and Rac-dependent assembly of focal adhesion complexes and actin filaments in permeabilized fibroblasts: an essential role for ezrin/radixin/moesin proteins. J. Cell Biol. *138*, 927–938.

Matsui, T., Maeda, M., Doi, Y., Yonemura, S., Amano, M., Kaibuchi, K., Tsukita, S., and Tsukita, S. (1998). Rho-kinase phosphorylates COOH-terminal threonines of ezrin/radixin/moesin (ERM) proteins and regulates their head-to-tail association. J. Cell Biol. *140*, 647–657.

Matsui, T., Yonemura, S., Tsukita, S., and Tsukita, S. (1999). Activation of ERM proteins in vivo by Rho involves phosphatidyl-inositol 4-phosphate 5-kinase and not ROCK kinases. Curr. Biol. *9*, 1259–1262.

May, V., Schiller, M. R., Eipper, B. A., and Mains, R. E. (2002). Kalirin Dbl-homology guanine nucleotide exchange factor 1 domain initiates new axon outgrowths via RhoG-mediated mechanisms. J. Neurosci. *22*, 6980–6990.

Nijhara, R., van Hennik, P. B., Gignac, M. L., Kruhlak, M. J., Hordijk, P. L., Delon, J., and Shaw, S. (2004). Rac1 mediates collapse of microvilli on chemokine-activated T lymphocytes. J. Immunol. *173*, 4985–4993.

Patel, J. C., and Galan, J. E. (2006). Differential activation and function of Rho GTPases during *Salmonella*-host cell interactions. J. Cell Biol. *175*, 453–463.

Prieto-Sanchez, R. M., and Bustelo, X. R. (2003). Structural basis for the signaling specificity of RhoG and Rac1 GTPases. J. Biol. Chem. *278*, 37916–37925.

Pujuguet, P., Del Maestro, L., Gautreau, A., Louvard, D., and Arpin, M. (2003). Ezrin regulates E-cadherin-dependent adherens junction assembly through Rac1 activation. Mol. Biol. Cell *14*, 2181–2191.

Ridley, A. J., Paterson, H. F., Johnston, C. L., Diekmann, D., and Hall, A. (1992). The small GTP-binding protein rac regulates growth factor-induced membrane ruffling. Cell *70*, 401–410.

Rossman, K. L., Der, C. J., and Sondek, J. (2005). GEF means go: turning on RHO GTPases with guanine nucleotide-exchange factors. Nat. Rev. Mol. Cell Biol. *6*, 167–180.

Saotome, I., Curto, M., and McClatchey, A. I. (2004). Ezrin is essential for epithelial organization and villus morphogenesis in the developing intestine. Dev. Cell *6*, 855–864.

Schiller, M. R., Blangy, A., Huang, J., Mains, R. E., and Eipper, B. A. (2005). Induction of lamellipodia by Kalirin does not require its guanine nucleotide exchange factor activity. Exp. Cell Res. *307*, 402–417.

Schmidt, A., and Hall, A. (2002). Guanine nucleotide exchange factors for Rho GTPases: turning on the switch. Genes Dev. *16*, 1587–1609.

Speck, O., Hughes, S. C., Noren, N. K., Kulikauskas, R. M., and Fehon, R. G. (2003). Moesin functions antagonistically to the Rho pathway to maintain epithelial integrity. Nature *421*, 83–87.

Srivastava, J., Elliott, B. E., Louvard, D., and Arpin, M. (2005). Src-dependent ezrin phosphorylation in adhesion-mediated signaling. Mol. Biol. Cell *16*, 1481–1490.

Takahashi, K., Sasaki, T., Mammoto, A., Hotta, I., Takaishi, K., Imamura, M., Nakano, K., Kodama, A., and Takai, Y. (1998). Interaction of radixin with Rho small G protein GDP/GTP exchange protein Dbl. Oncogene *16*, 3279–3284.

Takahashi, K., Sasaki, T., Mammoto, A., Takaishi, K., Kameyama, T., Tsukita, S., Tsukita, S., and Takai, Y. (1997). Direct interaction of the Rho GDP dissociation inhibitor with ezrin/radixin/moesin initiates the activation of the Rho small G protein. J. Biol. Chem. *272*, 23371–23375.

Tamura, A., Kikuchi, S., Hata, M., Katsuno, T., Matsui, T., Hayashi, H., Suzuki, Y., Noda, T., and Tsukita, S. (2005). Achlorhydria by ezrin knockdown: defects in the formation/expansion of apical canaliculi in gastric parietal cells. J. Cell Biol. *169*, 21–28.

Thompson, G., Owen, D., Chalk, P. A., and Lowe, P. N. (1998). Delineation of the Cdc42/Rac-binding domain of p21-activated kinase. Biochemistry *37*, 7885–7891.

Tirode, F., Malaguti, C., Romero, F., Attar, R., Camonis, J., and Egly, J. M. (1997). A conditionally expressed third partner stabilizes or prevents the formation of a transcriptional activator in a three-hybrid system. J. Biol. Chem. *272*, 22995–22999.

Turunen, O., Wahlström, T., and Vaheri, A. (1994). Ezrin has a COOH-terminal actin-binding site that is conserved in the ezrin protein family. J. Cell Biol. *126*, 1445–1453.

Vanni, C., Parodi, A., Mancini, P., Visco, V., Ottaviano, C., Torrisi, M. R., and Eva, A. (2004). Phosphorylation-independent membrane relocalization of ezrin following association with Dbl in vivo. Oncogene *23*, 4098–4106.

Wang, L., Zhu, K., and Zheng, Y. (2004). Oncogenic Dbl, Cdc42, and p21-activated kinase form a ternary signaling intermediate through the minimum interactive domains. Biochemistry *43*, 14584–14593.

Wennerberg, K., Ellerbroek, S. M., Liu, R. Y., Karnoub, A. E., Burridge, K., and Der, C. J. (2002). RhoG signals in parallel with Rac1 and Cdc42. J. Biol. Chem. *277*, 47810–47817.

West, M. A., Bretscher, M. S., and Watts, C. (1989). Distinct endocytotic pathways in epidermal growth factor-stimulated human carcinoma A431 cells. J. Cell Biol. *109*, 2731–2739.

Whitehead, I. P., Campbell, S., Rossman, K. L., and Der, C. J. (1997). Dbl family proteins. Biochim. Biophys. Acta *1332*, F1–F23.

Wigler, M., Silverstein, S., Lee, L. S., Pellicer, A., Cheng, Y., and Axel, R. (1977). Transfer of purified herpes virus thymidine kinase gene to cultured mouse cells. Cell *11*, 223–232.

Wu, Y. C., Tsai, M. C., Cheng, L. C., Chou, C. J., and Weng, N. Y. (2001). *C. elegans* CED-12 acts in the conserved crkII/DOCK180/Rac pathway to control cell migration and cell corpse engulfment. Dev. Cell *1*, 491–502.

Yonemura, S., Matsui, T., Tsukita, S., and Tsukita, S. (2002). Rho-dependent and -independent activation mechanisms of ezrin/radixin/moesin proteins: an essential role for polyphosphoinositides in vivo. J. Cell Sci. *115*, 2569–2580.